Characterisation of LEDs with a Michelson Interferometer

Muchen Li
Blackett Laboratory, Imperial College London
(Dated: 01 February 2019)

We use a Michelson interferometer as a Fourier transform spectrometer to complete spectroscopic tasks on blue and white LEDs. Direct interferogram analysis shows the blue LED's spectrum is well described by a Gaussian, with mean wavelength $\bar{\lambda} = (462.3 \pm 0.4)$ nm, spectral width $\sigma_{\bar{\lambda}} = (9.4 \pm 0.3)$ nm, and coherent length $\sigma_d = (1.81 \pm 0.05)$ μm. The white LED was hypothesised to be a blue LED with phosphor coating that absorbs blue and emits broad Gaussian yellow light. This is confirmed by the FFT results $\bar{\lambda}^{\text{blue}} = (459.8 \pm 0.3)$ nm, $\sigma_{\bar{\lambda}}{}^{\text{blue}} = (10.5 \pm 0.3)$ nm, $\bar{\lambda}^{\text{yellow}} = (579.5 \pm 1.2)$ nm, and $\sigma_{\bar{\lambda}}{}^{\text{yellow}} = (63.5 \pm 1.3)$ nm, where we take into account the spectral sensitivity of the photodiode.

I. Introduction

The Michelson interferometer is one of the most important apparatuses in optical interferometry, with a wide range of applications. One such application is using the interferometer as a *Fourier transform spectrometer*, which determines the spectrum of a given light source.

In this experiment, we investigate the characteristics of two LEDs using a Michelson interferometer. The interferometer splits and recombines a given beam, and outputs the resulting interference pattern as an intensity–distance (or path difference) plot. The plot (signal, or interferogram) encodes essential information about the light source as it is a Fourier transform of the wavelength spectrum [1].

Using both direct analysis on the signal, and the Fast Fourier Transform (FFT), we determine the mean wavelengths, coherent lengths, and the spectral widths of light emitted by blue and white LEDs. The experimental results are compared against predictions made from consideration of mechanisms responsible for producing the sources' light.

Analysis of light emission spectra is particularly important as it yields information about the matter producing these spectra: for example, the atomic composition of nearby stars. Compared to the traditional diffraction grating, which directly returns the desired spectrum across a semicircle [1], the Fourier transform spectrometer is more accurate, flexible, and yields spectra which are more complete.

II. Theory

Consider the amplitude sum A of two identical monochromatic light waves with amplitudes A_0, angular frequencies ω, and wavevectors $\mathbf{k}$ at some point $\mathbf{r}_0$:

$$A = A_0\left[e^{i(\omega t + \mathbf{k}\cdot\mathbf{r}_0)} + e^{i(\omega t + \mathbf{k}\cdot\mathbf{r}_0 + \phi)}\right] , \tag{2.1}$$

where ϕ is the phase difference between the beams, which is related to the path difference Δ and $k = |\mathbf{k}|$ as

$$\phi = k\Delta . \tag{2.2}$$

The total intensity is therefore

$$I = |A|^2 = I_0(1 + \cos k\Delta) , \tag{2.3}$$

or equivalently

$$\tilde{I} = I_0(1 + e^{ik\Delta}) , \tag{2.4}$$

where we define $I_0 = 2{A_0}^2$ as the individual intensities, and $I = \mathrm{Re}\big(\tilde{I}\big)$.

If the light waves have a spectrum given by $I_0(k)$ instead, then the total intensity at $\mathbf{r}_0$ is the sum of (2.4) over all k:

$$\tilde{I}(\Delta) = \int_0^\infty I_0(k)(1 + e^{ik\Delta})\,\mathrm{d}k . \tag{2.5}$$

The first integral is the constant background intensity I_b due to the interference of all wavenumbers, which are incoherent; the second is a Fourier transform of $I_0(k)$. Rewriting (2.5) as

$$\tilde{I}(\Delta) = I_\mathrm{b} + \mathcal{F}[I_0(k)] \tag{2.6}$$

explicitly shows that $\tilde{I}(\Delta)$ and $I_0(k)$ are Fourier transform pairs to within a constant. Therefore, given a known real signal $I(\Delta)$, the desired spectrum $I_0(k)$ can be found by evaluating

$$I_0(k > 0) = \mathrm{Re}\Big[\mathcal{F}^{-1}[I(\Delta) - I_\mathrm{b}]\Big] . \tag{2.7}$$

The measured signal $I(\Delta)$ consists of discrete data points, so we use Python's FFT package to transform it into $I_0(k)$. Although we can analyse any given signal with FFT, it is sometimes not the most accurate technique, as FFT produce peaks in spectra which contain a small fraction of data points. Sometimes, a more suitable technique is analysing the signal directly, as certain Fourier transform pairs are very well known.

The two important (real parts of) Fourier pairs for this experiment are

$$\cos(k_0\Delta) \rightleftharpoons \delta(k-k_0) \ ; \tag{2.8}$$

$$\cos(k_0\Delta)\exp\left(\frac{-\Delta^2}{2\sigma^2}\right) \rightleftharpoons \frac{\sigma}{\sqrt{2\pi}}\exp\left[\frac{-\sigma^2(k-k_0)^2}{2}\right] \ , \tag{2.9}$$

where σ and k_0 are constants [2]. Eqn. (2.8) shows that if the light is monochromatic, simple (co)sinusoids of wavevector k_0 will be observed. However, infinitely pure spectra cannot really exist. Real spectra contain peaks which can generally be described by Gaussians with a standard deviation σ [3]. Here, (2.9) shows the signal observed will be another Gaussian with standard deviation σ^{-1} enveloping the (co)sinusoids.

III. Method

We set up the Michelson interferometer shown in Fig. 1 on an optical table.

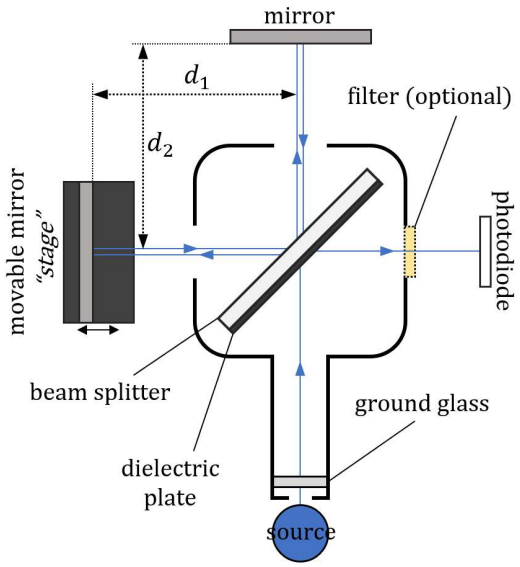

FIG. 1. A diagram showing the setup of our Michelson interferometer. Light beam from the source is split and recombined, after being reflected by the two mirrors. The photodiode records the intensity of the recombined light. The stage's movement is controlled by a computer. The ground glass serves as a light diffuser so the field behind it is as evenly illuminated as possible. The dielectric plate induces a 180° phase change for one of the beams.

If the left transmitted beam is slightly tilted when incident on the stage, then its movement would cause a different, nearby part of the beam to be recombined with the top beam. For sources with relatively uniform intensity across their beams, misalignment effects are negligible. However, for non-uniform sources, unwanted artefacts would be induced into the signal.

To minimise misalignment, we firstly attached and adjusted the unit containing the beam splitter and dielectric plate. We used the white LED as the source, since it was found to be particularly non-uniform (Section IV.B), which is useful for amplifying misalignment effects. The stage was run across its maximum range quickly, and the signal observed. The stage tilt and the unit's orientation were adjusted, and the process repeated until the signal observed was approximately constant.

The other mirror was then attached, with $d_1 \approx d_2$. We now use an expanded green laser as the source, as the light is very intense and monochromatic, which is useful for observing fringes. The mirror was adjusted until Haidinger (circular) fringes, which arises due to cylindrical symmetry of a correctly aligned setup, can be seen at the place of the photodiode, and that the fringes were centred in the middle of the beam. The stage was rerun to ensure these conditions were met across its maximum range.

Lastly, we found the **null point**, which is the position of the stage where $d_1 = d_2$ exactly, or $\Delta = 0$. The laser and lens were removed; the photodiode and white LED attached. We ran the stage over its maximum range at 100 μm/s, with a data collection frequency of 50 Hz, such that interference patterns around $\Delta = 0$ are clearly visible, but the scan takes only ~3 minutes. Once signals emerged from noise over a short range, we scanned over this range at reduced speeds, and found the null point where maximum *destructive* (due to the dielectric plate) interference occurs, to 4 significant figures.

The ground glass was attached, and data collection then completed with the appropriate sources, filters and scans around the null point. We use the stage speed 0.1 μm/s at the same data collection frequency, such that ~100 data points are collected per half-wavelength.

IV. Results and Discussion

We present results in wavelengths here, rather than wavenumbers. The relationship between a wavelength difference $\delta\lambda = \lambda_2 - \lambda_1$ and its wavenumber difference $\delta k = k_2 - k_1$ is:

$$|\delta k| = \frac{2\pi}{\lambda_1\lambda_2}|\delta\lambda| \ . \tag{4.1}$$

Consider a Gaussian *spectrum* centred at $\bar{\lambda} = 2\pi\bar{k}^{-1}$, with standard deviation $\sigma_{\bar{\lambda}}$. We define $\bar{\lambda}$ as the **mean wavelength**, and $\sigma_{\bar{\lambda}}$ as the **spectral width** of this Gaussian. Eqn. (4.1) can thus be rewritten as

$$\sigma_{\bar{k}} = \frac{2\pi}{\left(\bar{\lambda}+\frac{\sigma_{\bar{\lambda}}}{2}\right)\left(\bar{\lambda}-\frac{\sigma_{\bar{\lambda}}}{2}\right)}\sigma_{\bar{\lambda}} \ , \tag{4.2}$$

where $\sigma_{\bar{k}}$ is the wavenumber spectral width.

From (2.9), the relationship between $\sigma_{\bar{k}}$, and σ_Δ, the standard deviation of the Gaussian in the *signal, with* Δ *on the x-axis*, is:

$$\sigma_{\bar{k}}\sigma_\Delta = 1 \ . \tag{4.3}$$

We define

$$\sigma_d = \frac{\sigma_\Delta}{2} \tag{4.4}$$

as the Gaussian's **coherent length**, as the *distance* from null point d is related to Δ by $\Delta = 2d$, and signals in general have d on the x-axis.

Solving (4.2) therefore yields

$$\sigma_{\bar\lambda} = \sqrt{64\pi^2{\sigma_d}^2 + 4\bar\lambda^2} - 8\pi\sigma_d \ , \tag{4.5}$$

which allows the conversion of any coherent length into a spectral width.

A. Blue LED

We firstly analyse the blue LED light signal, with a shape that matches (2.9), shown in Fig. 2.

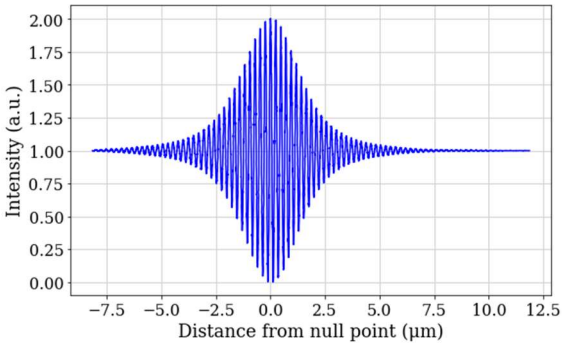

FIG. 2. The blue LED signal. The x-axis is distance, rather than path difference. The intensity is inverted (to remove the effect of the dielectric plate) and rescaled such that it is always greater than zero, and $I_\mathrm{b} = 1$ a. u.

We fit a simple sine wave to every n data points, such that all adjacent local maxima are fitted by slightly more than one sinusoid between them. Here, $n = 116$. The mean wavelength is determined as

$$\bar\lambda = (462.3 \pm 0.4) \text{ nm} \ , \tag{4.6}$$

where we took the **weighted mean** [4]

$$\bar\lambda = \frac{\sum \bar\lambda_i / {\sigma_i}^2}{\sum 1/{\sigma_i}^2} \tag{4.7}$$

with uncertainty

$$\varsigma_{\bar\lambda} = \sqrt{\frac{1}{\sum 1/{\sigma_i}^2}} \tag{4.8}$$

on the sinusoids' individual mean wavelengths $\bar\lambda_i$ and their uncertainties σ_i.

The coherent length is

$$\sigma_d = (1.81 \pm 0.05) \ \mu\text{m} \ , \tag{4.9}$$

which is the standard deviation of the Gaussian that fitted the sinusoids' amplitude plot. This fit is shown in Fig. 3.

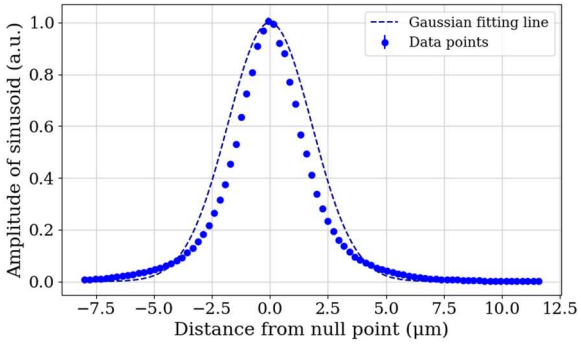

FIG. 3. A plot of the blue LED sinusoid fitting lines' amplitudes, and a Gaussian fitting line with free σ_d parameter. Although the Gaussian does not match the data completely, it is nonetheless a reasonable description for the amplitudes.

The spectral width is therefore

$$\sigma_{\bar\lambda} = (9.4 \pm 0.3) \text{ nm} \ , \tag{4.10}$$

with the uncertainty calculated using the propagation of errors formula on (4.5). The error arises because the shape of the spectrum is not exactly Gaussian.

These results show whilst the spectral width is reasonably narrow, the light emitted is still not as pure as light from stimulated emissions in lasers or atomic transition emissions in gas discharge lamps, nor as broad as blackbody radiation. This makes sense as the light from a blue LED semiconductor is emitted due to electrons crossing the band gap, the difference in energy between top of the valence band and bottom of the conduction band [5]. The light is impure because the band gap is the *minimum* energy that an electron could lose in crossing to the valence band.

The spectrum of the light shown in Fig. 4 is also obtained using FFT on the signal. The photodiode has a non-uniform spectral sensitivity S_rel profile [6], shown in Fig. 5. We approximate this profile by

$$S_\mathrm{rel} = \begin{cases} \dfrac{\lambda}{700} - \dfrac{11}{35} & \text{if } 220 < \lambda \le 920 \\ \dfrac{91\lambda}{2000} - \dfrac{\lambda^2}{40000} - \dfrac{197}{10} & \text{if } 920 < \lambda \le 1110 \\ 0 & \text{otherwise} \end{cases} \ , \tag{4.11}$$

where λ is in nm. The original FFT spectrum is corrected by dividing by (4.11) to produce Fig. 4.

The shape of the spectrum matches well with the prediction that it is approximately Gaussian. The quantities extracted from Fig. 4:

$$\bar\lambda = (467.6 \pm 0.5) \text{ nm} \ ; \tag{4.12}$$

$$\sigma_{\bar\lambda} = (12.3 \pm 0.5) \text{ nm} \tag{4.13}$$

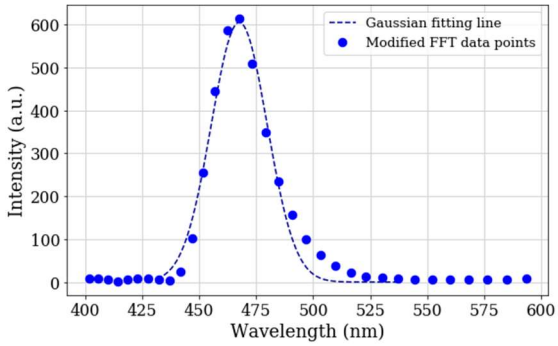

FIG. 4. The corrected blue LED FFT profile, with a free Gaussian fitting line. There are artefacts in the low (~50 nm) wavelength regions (not shown here) due to erratic movement of the stage at low speeds, producing clustered data.

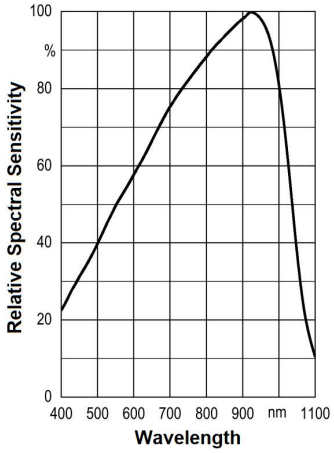

FIG. 5. [6] The photodiode spectral sensitivity profile.

agree reasonably well with values in (4.6) and (4.10). These quantities were obtained by a Gaussian fit to the corrected FFT data near the peak, also shown in Fig. 4.

B. White LED

Before we scanned the white LED, it was shone onto a black wall from a distance. Two interesting features were observed: blue hues in certain regions, and a non-uniform intensity profile for the remaining regions.

White LEDs conventionally produce light by one of two methods: the first is the mixture of red, green, and blue LEDs; the second is the through scintillation of light emitted by a blue LED: some of its light is absorbed by a phosphor layer and re-emitted in the yellow wavelengths, with a relatively wide spectrum that encompasses much of the visible range [5].

We hypothesise, based on the earlier observation, that our white LED was a phosphor scintillation LED. The latter observation suggests the LED was a non-uniform source, which explains the asymmetries observed in the signal, shown in Fig. 6. The signal displays some limited beating behaviour.

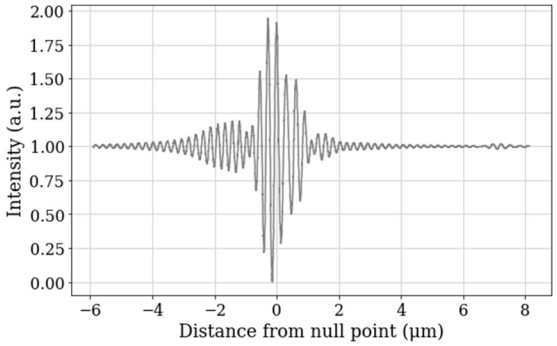

FIG. 6. The white LED light signal. Note the asymmetries due to the non-uniform source and slight misalignments in the interferometer.

The coherent length is approximately

$$\sigma_d = (0.53 \pm 0.08)\ \mu\text{m}\ , \tag{4.14}$$

determined using a Gaussian fit on the fitting sinusoids' amplitudes. Here, $n = 118$.

Due to asymmetries affecting the anticipated beating behaviour, it is inappropriate to proceed using signal analysis. Instead, we take a corrected FFT. The resulting spectrum is shown in Fig. 7. Note that one Gaussian in the spectrum overlaps reasonably well with the blue LED's.

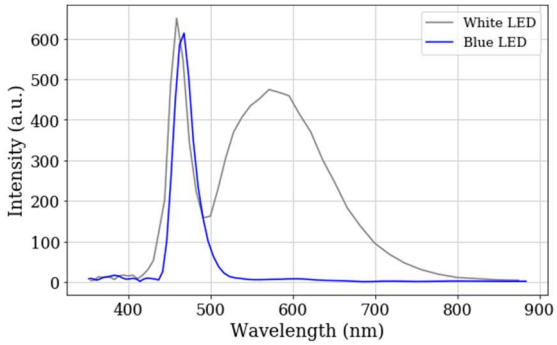

FIG. 7. The corrected FFT profiles for both LEDs.

The mean wavelengths and spectral widths of the two Gaussians are

$$\bar{\lambda}^{\text{blue}} = (459.8 \pm 0.3)\ \text{nm}\ ; \tag{4.15}$$

$$\sigma_{\bar{\lambda}}{}^{\text{blue}} = (10.5 \pm 0.3)\ \text{nm}\ ; \tag{4.16}$$

$$\bar{\lambda}^{\text{yellow}} = (579.5 \pm 1.2)\ \text{nm}\ ; \tag{4.17}$$

$$\sigma_{\bar{\lambda}}{}^{\text{yellow}} = (63.5 \pm 1.3)\ \text{nm}\ , \tag{4.18}$$

where we fit two separate Gaussians to the corrected FFT data shown in Fig. 8. These results confirm our hypothesis.

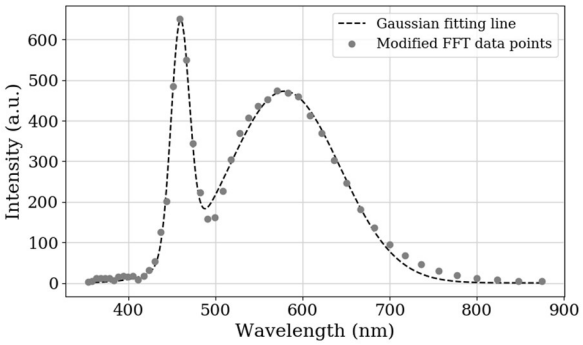

FIG. 8. The corrected white LED FFT profile, with a fitting line that is the sum of two free Gaussians.

V. Conclusions

We found, by signal analysis, that the blue LED's spectrum was well approximated by a Gaussian with mean $\bar{\lambda} = (462.3 \pm 0.4)$ nm and standard deviation $\sigma_{\bar{\lambda}} = (9.4 \pm 0.3)$ nm. A corrected FFT showed $\bar{\lambda} = (467.6 \pm 0.5)$ nm and $\sigma_{\bar{\lambda}} = (12.3 \pm 0.5)$ nm, which agreed reasonably with the earlier results. The white LED was found to be a phosphor scintillation LED with dual Gaussian spectrum $\bar{\lambda}^{\text{blue}} = (459.8 \pm 0.3)$ nm, ${\sigma_{\bar{\lambda}}}^{\text{blue}} = (10.5 \pm 0.3)$ nm, $\bar{\lambda}^{\text{yellow}} = (579.5 \pm 1.2)$ nm, and ${\sigma_{\bar{\lambda}}}^{\text{yellow}} = (63.5 \pm 1.3)$ nm. The coherent lengths were found as $\sigma_d = (1.81 \pm 0.05)$ μm and (0.53 ± 0.08) μm for the blue and white LEDs, respectively.

Improvements to our interferometer would allow more accurate signals to be detected, and very delicate effects like the Zeeman effect to be observed. Our photodiode was not particularly suited for advanced spectroscopic tasks, as it had a non-uniform spectral sensitivity profile which differed dependent on manufacturing conditions and is ill equipped to detect light outside of the visible and near infrared regions. Specially made CCD cameras are far better alternatives. In addition, the erratic stage movement at low speeds is prohibitive for precise FFT plots. A better designed motor which does not rely on magnets would significantly improve the quality of results, and the flexibility of the spectrometer.

References

[1] Hecht E. *Optics*. 4th ed. United Kingdom: Pearson Education; 2014.

[2] Arfken GB, Weber HJ, Harris FE. *Mathematical Methods for Physicists: A Comprehensive Guide*. 7th ed. USA: Elsevier; 2013.

[3] Colling DJ. *Second Year Laboratory: Interferometry*. London: Imperial College London; 2019. Available from: https://www.imperial.ac.uk/media/imperial-college/faculty-of-natural-sciences/department-of-physics/ug-labs/year-2/labscripts/Interferometry_0.3.1.pdf [Accessed 01 February 2019].

[4] Leo WR. *Statistics and the Treatment of Experimental Data*. 2003. Available from: https://ned.ipac.caltech.edu/level5/Leo/paper.pdf [Accessed 01 February 2019].

[5] Sze SM, Ng KK. *Physics of Semiconductor Devices*. New Jersey: John Wiley & Sons; 2007.

[6] OSRAM Opto Semiconductors. *Silicon PIN Photodiode*. Version 1.3. Regensburg: OSRAM Opto Semiconductors; 2017. Available from: https://www.osram.com/media/resource/hires/osram-dam-2495983/SFH%202200.pdf [Accessed 01 February 2019].